NASA Technical Memorandum 101573

TIME-CORRELATED GUST LOADS USING MATCHED-FILTER THEORY AND RANDOM-PROCESS THEORY - A NEW WAY OF LOOKING AT THINGS

Anthony S. Pototzky, Thomas A. Zeiler, and Boyd Perry III

APRIL 1989

National Aeronautics and Space Administration

Langley Research Center
Hampton, Virginia 23665-5225

Time - Correlated Gust Loads Using Matched Filter Theory and Random Process Theory - A New Way of Looking at Things

by

Anthony S. Pototzky* and Thomas A. Zeiler**
Planning Research Corporation
Aerospace Technologies Division
Hanption, Virginia 23666

and

Boyd Perry, III***
Langley Research Center
National Aeronautics and Space Administration
Hampton, Virginia 23665

Abstract

This paper describes and illustrates two ways of performing time-correlated gust-load calculations. The first is based on Matched Filter Theory; the second on Random Process Theory. Both approaches yield theoretically identical results and represent novel applications of the theories, are computationally fast, and may be applied to other dynamic-response problems. A theoretical development and example calculations using both Matched Filter Theory and Random Process Theory approaches are presented.

Nomenclature

Roman

$G(s)$	transfer function of vertical velocity component of von Karman turbulence (gust)
$h_i(t)$	time response of output variable i to unit impulse
$H_i(\omega)$	frequency response function of output variable i
K	arbitrary constant
L	scale of turbulence in G(s), equation (11)
$R_{ij}(\tau)$	cross-correlation function between quantities i and j; auto-correlation function if i equals j
s	Laplace variable
$S_{ij}(\omega)$	cross-power spectral density function between quantities i and j; auto-power spectral density function if i equals j
t	time
t_o	arbitrary time shift
V	velocity of aircraft in equation (11)
$w_g(t)$	vertical velocity component of gust
$W_g(\omega)$	Fourier transform of $w_g(t)$
$x(t)$	"matched" excitation waveform
$X(\omega)$	Fourier transform of x(t)
$y(t)$	time response of output quantity y
$y_y(t)$	time response of output quantity y to excitation matched to y
$y_z(t)$	time response of output quantity y to excitation matched to z
$Y(\omega)$	Fourier transform of y(t)
$z(t)$	time response of output quantity z
$z_y(t)$	time response of output quantity z to excitation matched to y
$z_z(t)$	time response of output quantity z to excitation matched to z
$Z(\omega)$	Fourier transform of z(t)

Greek

σ_i	root-mean-square of quantity i
τ	time argument for auto- and cross-correlation functions
ω	circular frequency (rad/sec)

Superscripts

*	complex conjugate

Subscripts

g	gust
h	unit impulse time response
x	matched excitation waveform

---

* Engineering Specialist, Member AIAA

** Project Structures Engineer, Member AIAA

*** Aerospace Engineer

y response quantity y

z response quantity z

Introduction

The primary structure of an aircraft must withstand all the static and dynamic loads it is expected to encounter during its life. Such loads include landing and taxi loads, maneuver loads, and gust loads. There are several methods used by airframe manufacturers to compute gust loads to satisfy certification requirements and include both stochastic methods and deterministic methods. The U.S. Federal Aviation Administration (FAA) recently asked the National Aeronautics and Space Administration (NASA) for assistance in evaluating the Statistical Discrete Gust (SDG) Method [1] as a candidate gust-loads analysis method for complying with FAA certification requirements. The SDG method is a time-domain approach and yields time-correlated gust loads by employing a search procedure.

During the course of the NASA evaluation of the SDG method, the authors recognized that Matched Filter Theory (MFT) [2] could be applied to the linear gust problem to compute time-correlated gust loads. Computing time-correlated gust loads in this manner has the twin advantages of being computationally fast and of solving the problem directly. Historically, MFT was first utilized in the detection of returning radar signals. Papoulis [3] showed that the principles of MFT can be used to obtain maximized responses without the use of calculus of variations and in applications other than signal detection. The first purpose of this paper is to demonstrate that MFT is also applicable to aeroelastic systems, and specifically applicable to the computation of time-correlated gust loads.

During the course of the MFT investigation, the authors found that the maximized and as well as the other responses of the system looked similar to auto- and cross-correlation functions of Random Process Theory (RPT) [4]. From this observation and also from theoretical considerations given later, it was recognized that time-correlated gust loads computed by MFT are theoretically identical to those obtained using RPT. To the knowledge of the authors, the correlation functions of RPT have, until now, not been interpreted as time-correlated gust loads. Some preliminary analyses demonstrating this interpretation were presented by the authors in reference 5. The second purpose of this paper is to show the relationship between the results of MFT and RPT.

Both the MFT and the RPT procedures for computing time-correlated gust loads involve novel applications of the theories and unconventional interpretations of the intermediate and final results. This paper outlines the mathematical developments, recognizes a duality between MFT and RPT, and presents example calculations using both MFT and RPT for computing time-correlated gust loads.

Background

This section of the paper defines time-correlated gust loads and the current analysis capabilities in this area.

Time-Correlated Loads

This paper deals specifically with time-correlated gust loads and figure 1 illustrates two types of such loads. Time-correlated loads are time histories of two or more different load responses to the same disturbance quantity. In the figure the disturbance quantity is the vertical component of one-dimensional atmospheric turbulence and the time-correlated loads (the output quantities) are the resulting load responses (in this case the bending moments and torsion moments) at several locations on the airplane wing.

The first type of time-correlated load is illustrated on the right wing: loads (two bending moments in this illustration) at two different locations on the airplane. The second type is illustrated on the left wing: two different loads (bending moment and torsion moment in this illustration) at the same location on the airplane.

As indicated by the time histories in the figure, time correlation provides knowledge of the value (magnitude and sign) of one load when another is maximum (positive or negative). In general, the time correlation principle allows the computations of values of all loads at all the stations with respect to the time when any one maximum load occurred. Such information may be used directly during analyses and testing of aircraft structures [6].

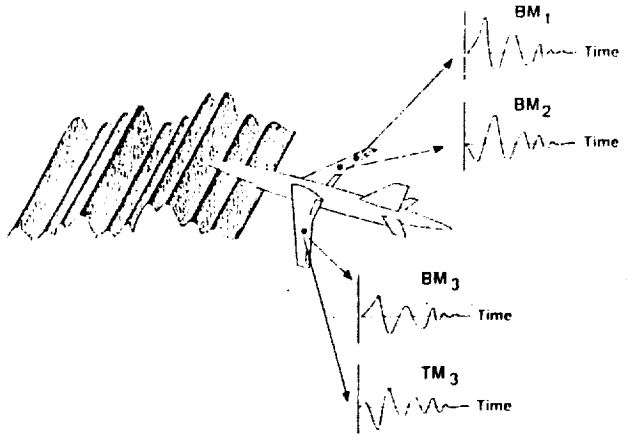

Figure 1. Time-Correlated Gust Loads

Statistical Discrete Gust Method

The SDG method determines the response time histories of "worst case" gust loads (such as shear forces, bending moments, and torsion moments) and the corresponding "critical gust profiles" which produce them. These loads are time correlated and this feature is a major advantage of the SDG method over some other gust loads analysis methods.

Another advantage of the SDG method is its applicability to nonlinear, as well as to linear, systems. The SDG method employs a search procedure to obtain its answers. For a linear system, by taking advantage of superposition, the search procedure may be simplified and reduced to a one-dimensional search. For a nonlinear system, however, this is not the case and the resulting search procedure remains multi-dimensional and can become computationally expensive [7].

Scope

In light of the technical contributions provided by the SDG method as outlined above, this section states the conditions under which and the means by which this paper makes a contribution to the area of time-correlated gust-load calculations: (a) the SDG method is capable of performing both linear and nonlinear analyses, whereas the present methods are restricted to linear systems only; (b) the SDG method uses a search procedure, whereas the present methods obtain the same quantities directly and with a significant reduction in computation time.

Theoretical Development

In this section the theoretical background of the MFT and RPT approaches will be presented. For this paper, the Fourier transform of a function f(t) is defined by,

$$F(\omega) = \int_{-\infty}^{\infty} f(t)\, e^{-i\omega t}\, dt,$$

and the inverse Fourier transform is given by,

$$f(t) = \frac{1}{2\pi} \int_{-\infty}^{\infty} F(\omega)\, e^{i\omega t}\, d\omega.$$

Matched Filter Theory Approach

The objective of MFT, as originally developed, is the design of an electronic filter such that its response to a *known* input signal is maximum at a specific time [3,8]. It found early application to radar considering the "filter" to be a *detector* that, in response to a known input signal, produces an output signal for further processing [2]. In this case the detector design is the optimum design for maximizing the output signal-to-noise ratio. The matched filter is designed so that the unit impulse response, $h_y(t)$, of the output y of the filter is proportional to the known signal, shifted and reversed in time,

$$h_y(t) = Kx(-t + t_o), \tag{1a}$$

where K is an arbitrary constant, t_o is an arbitrary time shift, and x(t) is the known input signal. As will be shown later, the time shift may be selected through criteria of convenience only and will be the time that the matched filter response is maximum.

In the present application, the filter is considered to be a system whose dynamics are known. Specifically, the system is characterized by the combination, in series, of the dynamics of atmospheric turbulence and the dynamics of aircraft load response. Thus $h_y(t)$ is known. The input signal, x(t), is to be determined from the impulse response of the system. From equation (1a),

$$x(t) = h_y(t_o - t)/K. \tag{1b}$$

The simple result of MFT allows direct determination of the input signal, or excitation, that produces a maximum response of the system. The result, as will be shown, is the maximum load response and the critical gust profile.

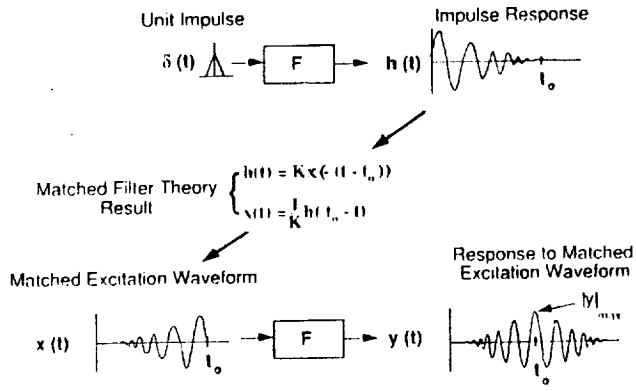

Figure 2. Matched Filter Theory - Signal Flow Diagram

Maximum Response to "Matched" Excitation Waveform - Equations (1a) and (1b) express the fundamental result of Matched Filter Theory and figure 2 illustrates the result: the response of the system "filter" to a unit impulse is proportional to the desired input waveform, x(t), when delayed by t_o and reversed in time. For convenience and to be consistent with references 3 and 8, the form given by equation (1a) will be used in the remainder of the theoretical development of the MFT approach. It should be pointed out that either form of the the equation will lead to the same final results.

The system response to x(t) may be obtained from the inverse Fourier transform

$$y(t) = \frac{1}{2\pi} \int_{-\infty}^{\infty} Y(\omega)\, e^{i\omega t}\, d\omega, \tag{2a}$$

where

$$Y(\omega) = H_y(\omega)\, X(\omega), \tag{2b}$$

and $H_y(\omega)$ and $X(\omega)$ are the Fourier transforms of $h_y(t)$ and x(t). $H_y(\omega)$, which is the frequency response function of the output y, may be determined from equation (1a) as

$$\begin{aligned} H_y(\omega) &= Ke^{-i\omega t_o} X(-\omega) \\ &= KX^*(\omega)\, e^{-i\omega t_o}. \end{aligned} \tag{3}$$

Thus the response y(t) is

$$y(t) = \frac{1}{2\pi} \int_{-\infty}^{\infty} KX^*(\omega)X(\omega)\, e^{i\omega(t - t_o)}\, d\omega. \tag{4}$$

Note that the product $X^*(\omega)\, X(\omega)$ is the energy spectrum or power spectral density (PSD), $S_{xx}(\omega)$, of x(t), and is an even function of frequency, so

$$y(t) = K \frac{1}{2\pi} \int_{-\infty}^{\infty} S_{xx}(\omega)\cos(\omega(t - t_o))\, d\omega. \tag{5a}$$

The maximum response occurs when $t = t_o$,

$$y_{max} = y(t_o) = K \left[\frac{1}{2\pi} \int_{-\infty}^{\infty} S_{xx}(\omega)\, d\omega \right]. \tag{5b}$$

It is convenient to set the term in brackets in equation (5b) equal to unity, which means that the root-mean-square (RMS) of the excitation waveform, x(t), is unity. That is,

$$\frac{1}{2\pi} \int_{-\infty}^{\infty} X^*(\omega)\, X(\omega)\, d\omega = \frac{1}{2\pi} \int_{-\infty}^{\infty} S_{xx}(\omega)\, d\omega = 1. \tag{6}$$

It can be shown that a necessary result of this assumption is that the arbitrary constant, K, is equal to the RMS of the impulse response, σ_{h_y}. The stipulation in equation (6) that the waveform be of unit energy will be used later as a constraint on all excitation waveforms considered and will provide a basis for comparison of their effects.

Finally, substituting for K in equations (5a) and (5b) gives,

$$y(t) = \sigma_{h_y} \frac{1}{2\pi} \int_{-\infty}^{\infty} S_{xx}(\omega) \cos(\omega(t - t_o)) \, d\omega \qquad (7a)$$

and

$$y_{max} = y(t_o) = \sigma_{h_y} . \qquad (7b)$$

The input x(t) is said to be "matched" to y, since x(t) is determined from the impulse response of y , equation (1), and will be referred to as the matched excitation waveform.

Response to Arbitrary Excitation Waveform - It can be shown that the response y'(t), say, of y to any arbitrary excitation, say x'(t), that satisfies the normalization constraint of equation (6), will never exceed the maximum, equation (7b), produced by the matched excitation, x(t). To see this, the Fourier transform of this response may be written

$$Y'(\omega) = H_y(\omega) \, X'(\omega) . \qquad (8)$$

Substituting equation (3) for $H_y(\omega)$ and taking the inverse Fourier transform gives

$$y'(t) = \frac{1}{2\pi} \int_{-\infty}^{\infty} \sigma_{h_y} X^*(\omega) X'(\omega) \, e^{i\omega(t - t_o)} \, d\omega . \qquad (9)$$

Applying Schwartz's Inequality to equation (9) gives

$$|y'(t)|^2 \le \sigma_{h_y}^2 \left[\frac{1}{2\pi} \int_{-\infty}^{\infty} X^*(\omega) X(\omega) \, d\omega \right] \times \left[\frac{1}{2\pi} \int_{-\infty}^{\infty} X'^*(\omega) X'(\omega) \, d\omega \right] . \qquad (10a)$$

Both bracketed terms equal unity because of the constraint, equation (6), imposed on the waveforms. Thus

$$|y'(t)| \le \sigma_{h_y} . \qquad (10b)$$

which states that the magnitude of the response of y to any excitation waveform (suitably normalized to satisfy equation (6)) never exceeds the maximum response to the excitation waveform that is matched to y.

Intermediate Results - Any given frequency response function can be built up from several separate ones and thus represent the combined effects of several subsystems. In the context of the present paper, a von Karman turbulence "pre-filter", represented by a transfer function, is implemented ahead of the aircraft response function. The turbulence transfer function used in this study is adapted from that obtained from reference 9,

$$G(s) = \sigma_g \sqrt{\frac{L}{\pi V}} \frac{(1 + 2.618 \frac{L}{V} s)(1 + 0.1298 \frac{L}{V} s)}{(1 + 2.083 \frac{L}{V} s)(1 + 0.823 \frac{L}{V} s)(1 + 0.0898 \frac{L}{V} s)} \qquad (11)$$

Thus, the transform of the response y, as expressed above in terms equation (2b), would be rewritten as,

$$Y(\omega) = \overline{H}_y(\omega) G(\omega) \, X(\omega) \qquad (12)$$

where

$$\overline{H}_y(\omega) G(\omega) = H_y(\omega) \qquad (13)$$

and $H_y(\omega)$ is the frequency response function of an aeroelastic system to turbulence. With the turbulence "pre-filter" known, the critical gust profile can be obtained as an intermediate result as

$$W_g(\omega) = G(\omega) X(\omega)$$

and from equations (3) and (13),

$$W_g(\omega) = \frac{1}{\sigma_{h_y}} G(\omega) G^*(\omega) \overline{H}_y^*(\omega) e^{-i\omega t_o} , \qquad (14a)$$

and taking the inverse Fourier Transform,

$$w_g(t) = \frac{1}{2\pi} \int_{-\infty}^{\infty} W_g(\omega) \, e^{i\omega t} d\omega$$

$$= \frac{1}{2\pi \sigma_{h_y}} \int_{-\infty}^{\infty} G(\omega) G^*(\omega) \overline{H}_y^*(\omega) e^{i\omega(t - t_o)} d\omega \qquad (14b)$$

This theoretical development was carried out in the context of the response of an aircraft to atmospheric turbulence, where the pre-filter represented the atmospheric turbulence. Theoretically, other pre-filters can be used to analyze responses to some other disturbance quantity. Potential alternative pre-filters include runway roughness, pilot dynamics, and control-surface deflections. The range of alternatives is limited only by the ingenuity of the analyst in developing appropriate pre-filters.

Duality Between MFT and RPT

Consider now two excitation waveforms $x_y(t)$ and $x_z(t)$ that are matched to two outputs, y and z, of a given system. The response of y to $x_z(t)$ is then

$$y_z(t) = \sigma_{h_y} \frac{1}{2\pi} \int_{-\infty}^{\infty} X_y^*(\omega) X_z(\omega) \, e^{i\omega(t - t_o)} \, d\omega . \qquad (15)$$

From equation (3),

$$X_y(\omega) = \frac{H_y^*(\omega)}{\sigma_{h_y}} e^{-i\omega t_o} \qquad (16a)$$

and

$$X_z(\omega) = \frac{H_z^*(\omega)}{\sigma_{h_z}} e^{-i\omega t_o} . \qquad (16b)$$

Thus,

$$y_z(t) = \frac{1}{\sigma_{h_z}} \frac{1}{2\pi} \int_{-\infty}^{\infty} H_y(\omega) H_z^*(\omega) \, e^{i\omega(t - t_o)} \, d\omega . \qquad (17)$$

The product $H_y(\omega) \, H_z^*(\omega)$ is the cross-PSD function, $S_{yz}(\omega)$, for outputs y and z, thus,

$$y_z(t) = \frac{1}{\sigma_{h_z}} \left[\frac{1}{2\pi} \int_{-\infty}^{\infty} S_{yz}(\omega) \, e^{i\omega(t - t_o)} \, d\omega \right] . \qquad (18)$$

The term in the brackets is the cross-correlation function, $R_{yz}(t - t_o)$, between outputs y and z [10], so,

$$y_z(t) = \frac{1}{\sigma_{h_z}} R_{yz}(t - t_o) . \qquad (19a)$$

Similarly, the response of z to $x_y(t)$ would be

$$z_y(t) = \frac{1}{\sigma_{h_y}} R_{zy}(t - t_o) , \qquad (19b)$$

where

$$R_{zy}(t - t_o) = \frac{1}{2\pi} \int_{-\infty}^{\infty} H_z(\omega) H_y^*(\omega) e^{i\omega(t - t_o)} d\omega$$

$$= \frac{1}{2\pi} \int_{-\infty}^{\infty} S_{zy}(\omega) e^{i\omega(t - t_o)} d\omega . \qquad (20)$$

Note also that these two cross-correlation functions satisfy the relation (where $\tau = t - t_o$),

$$R_{ij}(\tau) = R_{ji}(-\tau) .$$

Notice that if the response of y (or z) to its own matched excitation, $x_y(t)$ (or $x_z(t)$) were being considered, *auto*-PSD's (S_{yy} or S_{zz}) and *auto*-correlation functions (R_{yy} or R_{zz}) are involved. Thus, dynamic responses to various matched excitations are proportional to auto- and cross-correlation functions between the outputs. Further, when $t = t_o$,

$$y_y(t_o) = \frac{1}{\sigma_{h_y}} R_{yy}(0) . \qquad (21)$$

The auto-correlation function is an even function of its time argument, τ, and its value is maximum at $\tau = 0$ and is equal to the mean square of the PSD, S_{yy}. Thus,

$$y_y(t_o) = y_{max} = \sigma_{h_y} , \qquad (22)$$

which is the result obtained from the MFT approach, equation (7b).

The duality between MFT and RPT is apparent from comparison of equation (15), which results from the application of MFT, with equation (19), and from comparison of equation (7b) with equation (22). These equations show that the correlation functions of RPT can be interpreted as scaled time responses to the "matched" excitation waveforms of MFT; and, necessarily, that the value of the autocorrelation function at $\tau = 0$, $R_{yy}(0)$, is proportional to the maximum response, y_{max}, of MFT. The duality between MFT and RPT also allows a relationship to be established [11] between MFT and Phased Design Loads Analysis [6]. Further, since the product $G(\omega)G^*(\omega)$ in equation (14b) is equivalent to the von Karman turbulence PSD, the critical gust profile resulting from the matched excitation waveform can also be determined from

$$w_g(t) = \frac{1}{2\pi\sigma_{h_y}} \int_{-\infty}^{\infty} \Phi_g(\omega) \overline{H}_y^*(\omega) e^{i\omega(t - t_o)} d\omega . \qquad (23)$$

Thus, RPT, normally employed to determine the statistical properties of random processes, may also be employed to obtain certain deterministic responses provided that they are interpreted as responses to matched excitation waveforms as described by MFT. In circumstances for which no PSD is available (e.g. maneuvers) the MFT approach would have to be used. Actual implementation of the two approaches will be discussed presently.

Application of the Analysis Procedures to Time-Correlated Gust Loads

MFT Approach

Figure 3 contains a signal flow diagram of the steps necessary to generate a maximum dynamic response at some point in the aircraft structure. It is the mechanization of the information presented in the Theoretical Development section of the paper. The signal flow diagram is presented in two parts; the top half illustrates the generation of the system impulse response; the bottom half illustrates the generation of the maximum response of the system.

In the top half, the gust spectrum is excited by an impulse of unit strength to generate an intermediate gust impulse response which, in turn, is the excitation to the aircraft. Computationally, the time history of the impulse response is carried out until its magnitude dies out to a small fraction of the largest amplitude. Several output channels (y, z_1, ...) are shown in the figure, however, only one response (y) is used. This impulse response is then normalized according to equation (6a).

The bottom half illustrates how all the time-correlated responses are obtained including the maximum response of the output y, and the critical "gust" profile. The y response builds to a maximum at $t = t_o$ at which point the excitation ends. The response then decays to near zero. The maximum response, y_{max}, is equal to the RMS of the system impulse response. It should be mentioned that the responses shown for the other outputs are not maximized. The critical gust profile and maximum response of the system are unique to only one load output (the top output, y). For other maximum load responses a separate but similar analysis needs to be performed.

An important detail illustrated in this figure is the introduction of the a pre-filter. The effect of the pre-filter is to provide dynamics of the input disturbance which itself contributes to the shape and magnitude of "matched" excitation waveform. In this example, the pre-filter is an s-plane approximation of the von Karman spectrum, but in other applications it could be landing or taxiing disturbance dynamics or possibly "pilot" dynamics for maneuver loads.

RPT Approach

Figure 4 contains a signal flow diagram with two parts and is analogous to the diagram in figure 3. This figure illustrates the steps necessary to generate time-correlated gust loads using RPT. Whereas the signals in figure 3 were all in the time domain, all but one of the signals in this figure are in the frequency domain.

From the top half, the "Known Dynamics" box is the same as that in figure 3. The input to this box is Gaussian white noise and the output includes auto- and the cross-power spectral density functions of some aircraft response, with an intermediate output being the von Karman power spectral density function of atmospheric turbulence.

Time-correlated gust loads are obtained in the bottom half of the figure by taking the inverse Fourier transforms of the auto- and cross-power spectral density functions obtained in the top half. It should be mentioned that to obtain precise representations of the time-correlated loads it was necessary to deal numerically with two-sided spectra (that is, with both the positive and negative frequency components present).

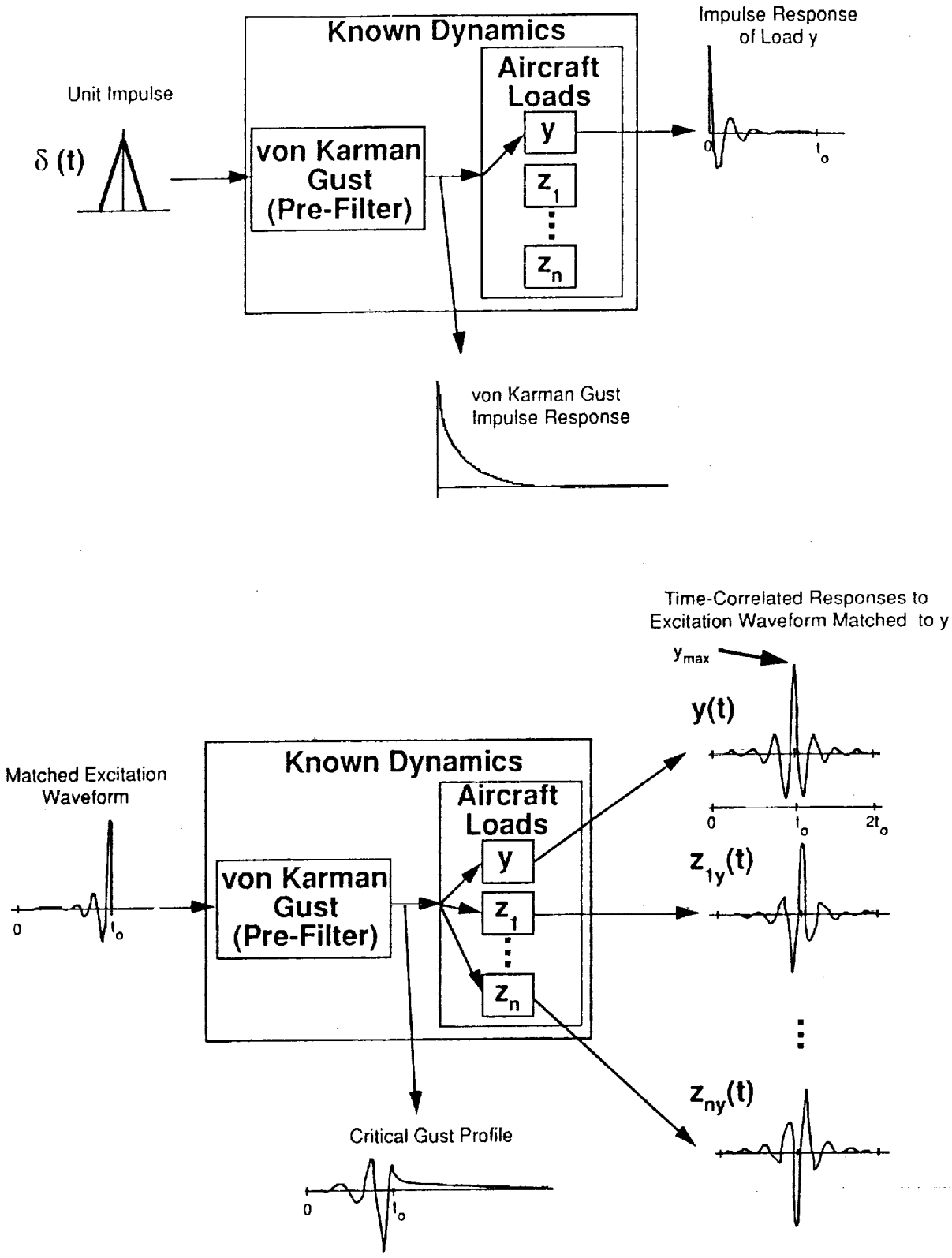

Figure 3. Implementation of Matched Filter Theory Approach - Signal Flow Diagram

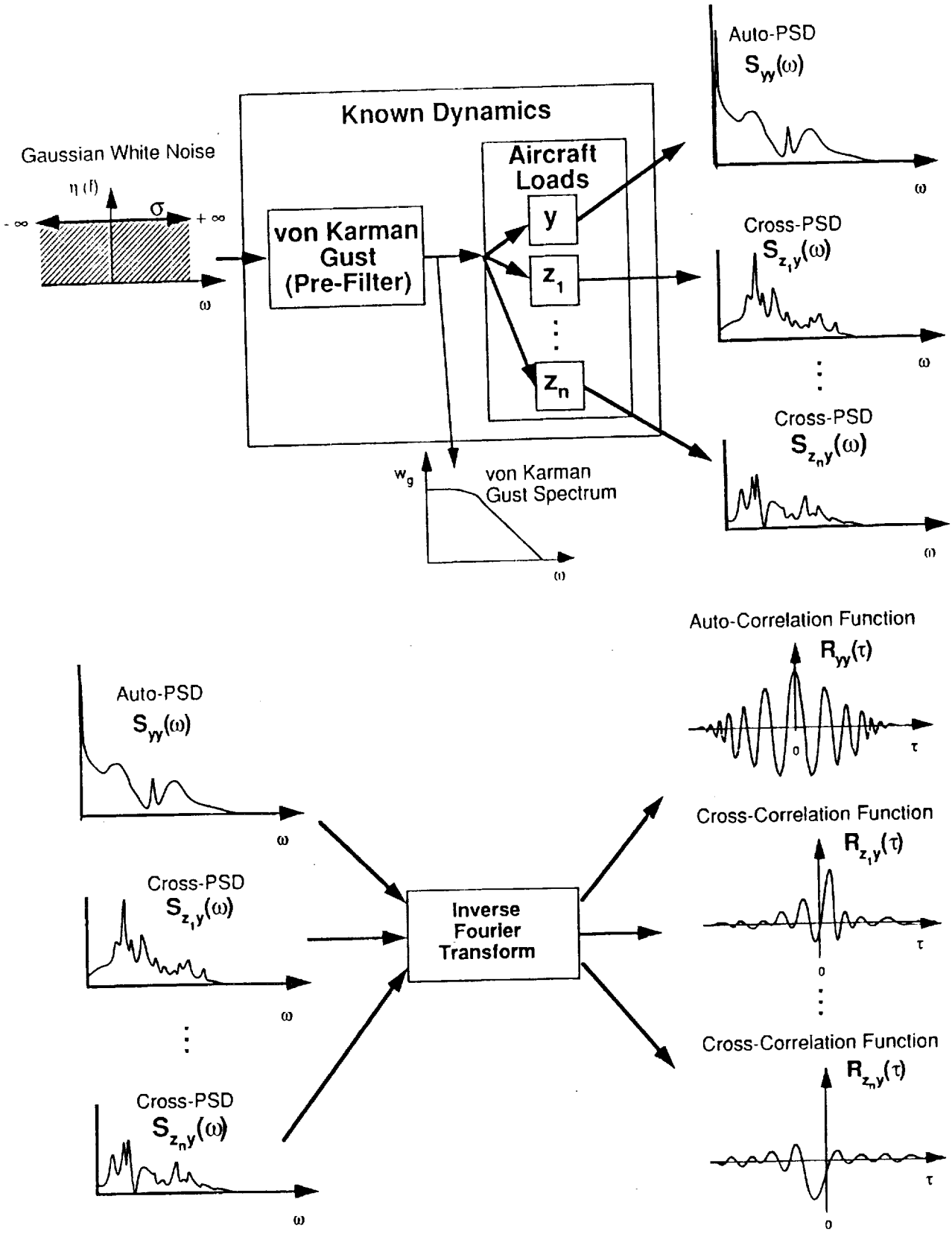

Figure 4. Implementation of Random Process Theory Approach - Signal Flow Diagram

Numerical Examples

Aeroelastic Configuration

In the application of MFT and RPT, existing structural and aerodynamic models of the NASA DAST ARW-2 were used. This configuration is a Firebee II target drone fitted with an Aeroelastic Research Wing (ARW) [12]. This model was especially well-suited for the study since it has structural flexibility, a stable and dominant short period, and several load outputs. The load outputs are comprised of shear forces, torsion moments, and bending moments at several points along the span of the wing. A detailed description of the dynamic loads model is available from reference 13.

Figure 5 shows some of the more important data of the vehicle itself and of the analytical representation of atmospheric turbulence. The structural part of the model was derived from a finite element code and the unsteady aerodynamics (at a Mach number of 0.7) from a doublet lattice code. Besides the two rigid-body modes, eight symmetric flexible modes were retained for this study. The final dynamics equations (the quadruple equations), constructed with a matrix analysis code, consisted of 97 first order equations, 9 output equations and one input. These final equations contained the dynamics of the structure, the of the unsteady aerodynamics, the loads, and the von Karman spectrum.

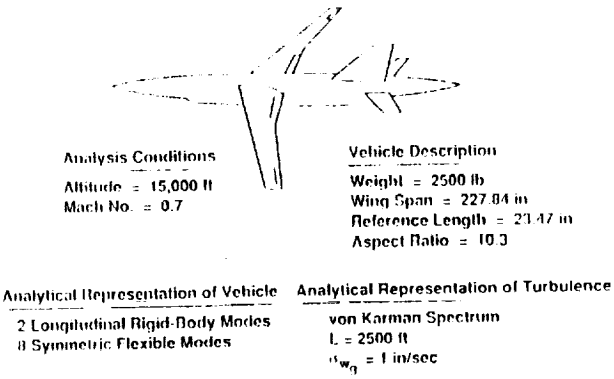

Figure 5. Aeroelastic Configuration - NASA DAST ARW-2

Time-Correlated Gust loads Using Matched Filter Theory

Figure 6 gives shows of the time-correlated loads at the wing root and the wing tip stations. The top two plots on the righthand side contain the time-histories of bending moment and torsion moment at the same root station on the structure. The top plot contains the bending moment response resulting from the excitation matched to root bending moment. The critical gust profile matched to the root bending moment is contained in the left plot. Although their magnitudes and signs may be different, the general shape of waveform represented by this plot is very similar for almost all the critical gust profiles of the system. The critical gust profile responses have the characteristic of being dominated by the short period dynamics of the aircraft. This phenomenon can be explained by examining equation (14a). The higher frequency aeroelastic responses due to the elastic modes are doubly attenuated by the high frequency roll-off of effectively two von Karman "pre-filters." The bottom righthand plot shows the time-history of bending moment response at a location near the tip of the wing.

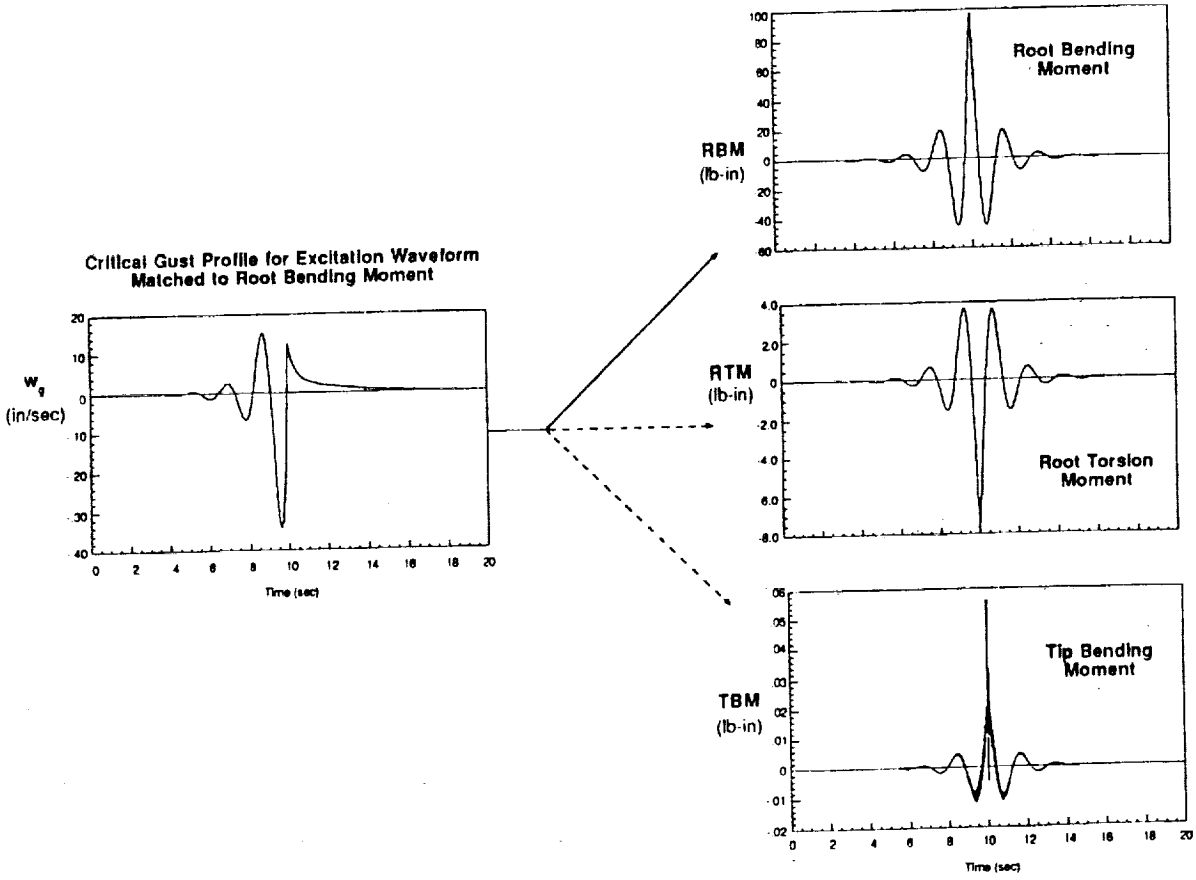

Figure 6. Time-Correlated Gust Loads - Matched Filter Theory Approach

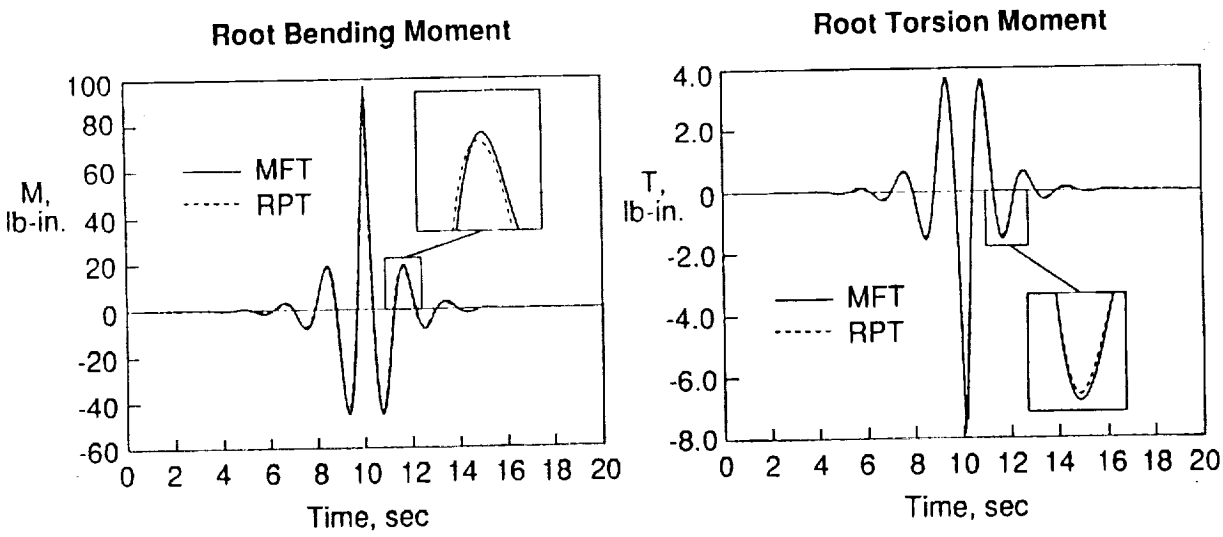

Figure 7. Comparison of MFT and RPT Calculations

Comparison of Results From MFT and RPT Calculations

Figure 7 shows a comparison of wing root bending moment and torsion moment time responses calculated with the MFT and RPT approaches. The Matched Filter Theory results are the same as those shown in figure 6. For purposes of comparison, the s-plane approximation of the von Karman gust power spectral density function is used for both the MFT and RPT calculations. Except for some slight differences in the peaks and troughs, results from the two approaches are practically indistinguishable. This is in accordance with the MFT/RPT duality described in the Theoretical Development section of the paper.

Concluding Remarks

This paper has described and illustrated two approaches for computing time-correlated gust loads. The two approaches yield theoretically identical results and are computationally fast. The first is based on Matched Filter Theory and is a time-domain approach; the second is based on Random Process Theory and is a frequency-domain approach. These approaches represent novel applications of the theories and unconventional interpretations of the intermediate and final results.

An important contribution of this paper is the introduction of a "pre-filter" in the application of Matched Filter Theory. The pre-filter is the mechanism by which the dynamics of the input disturbance (atmospheric turbulence) are incorporated into the problem and the resulting matched excitation waveform contains these dynamics. The output of the pre-filter due to the matched excitation waveform is the critical gust profile.

A second contribution of this paper is the interpretation of scaled correlation functions from Random Process Theory as time histories. It has been shown that the time-correlated gust loads predicted by Matched Filter Theory are theoretically identical to the auto- and cross-correlation functions, appropriately scaled, predicted by Random Process Theory. Further, the critical gust profile obtainable from the Matched Filter Theory approach is also obtainable from the Random Process Theory approach.

Although, in this paper, Matched Filter and Random Process Theories have been applied to the calculation of time-correlated gust loads, the approaches are general enough to be applied a variety of dynamic-response problems, such as taxi and landing loads, maneuver loads, and gust loads. The choice of which to use depends on the intended application.

References

1. Jones, J. G.: Statistical Discrete Gust Theory for Aircraft Loads. RAE Technical Report 73167, 1973.

2. North, Dwight O.: Analysis of the Factors Which Determine Signal/Noise Discrimination in Radar. RCA Laboratories, Princeton, New Jersey, Rept. PTR-6C, June, 1943.

3. Papoulis, Athanasios: Maximum Response With Input Energy Constraints and the Matched Filter Principle. *IEEE Transactions on Circuit Theory*, Vol. CT-17, No. 2, May, 1970, pp. 175 - 182.

4. Houbolt, John C.; Steiner, Roy; and Pratt, Kermit G.: Dynamic Response of Airplanes to Atmospheric Turbulence Including Flight Data on Input and Response. NASA TR -199,1964.

5. Pototzky, A. S.; Zeiler, T. A.; and Perry III, B.: Maximum Dynamic Responses Using Matched Filter Theory and Random Process Theory. NASA TM 100653, September 1988.

6. Moon, Richard N.: A Summary of Methods for Establishing Airframe Design Loads From Continuous Gust Design Criteria. Presented at the 65th AGARD Structures and Materials Panel, Turkey, October 4 - 9, 1987.

7. Noback, R.: S.D.G., P.S.D. and the Nonlinear Airplane. NLR MP 88018 U, Presented at the Gust Specialists Research Workshop, Williamsburg, Va., April 21, 1988.

8. Carlson, A. Bruce: *Communication Systems*, McGraw - Hill Book Company, New York, 1968.

9. Ly, Ui-Loi, personal communication, copy available from authors upon request.

10. Hardin, J. C.: *Introduction to Time Series Analysis*., NASA Reference Publication 1145, March,1986.

11. Zeiler, Thomas A.; and Pototzky, Anthony S.: On the Relationship Between Matched Filter Theory as Applied to Gust Loads and Phased Design Loads Analysis. NASA CR-181802, April 1989.

12. Murrow, H. N. and Eckstrom, C. V.: Drones for Aerodynamic and Structural Testing (DAST) - A Status Report. *AIAA Joural of Aircraft*, Vol. 16, No. 8, August 1979, pp. 521-526.

13. Pototzky, A. S. and Perry III, B.: New and Existing Techniques for Dynamic Loads Analyses of Flexible Airplanes. *AIAA Journal of Aircraft*, Vol. 23, No. 4, April, 1986, pp. 340-347.

NASA
National Aeronautics and Space Administration

Report Documentation Page

1. Report No.	2. Government Accession No.	3. Recipient's Catalog No.
NASA TM-101573		

4. Title and Subtitle

Time-Correlated Gust Loads Using Matched-Filter Theory and Random-Process Theory - A New Way of Looking at Things

5. Report Date

April 1989

6. Performing Organization Code

7. Author(s)

Anthony S. Pototzky
Thomas A. Zeiler
Boyd Perry III

8. Performing Organization Report No.

10. Work Unit No.

505-63-21-04

9. Performing Organization Name and Address

NASA Langley Research Center
Hampton, VA 23665-5225

11. Contract or Grant No.

13. Type of Report and Period Covered

Technical Memorandum

12. Sponsoring Agency Name and Address

National Aeronautics and Space Administration
Washington, DC 20546-0001

14. Sponsoring Agency Code

15. Supplementary Notes

Presented at the AIAA 30th Structures, Structural Dynamics and Materials Conference in Mobile, Alabama, April 3-5, 1989.

16. Abstract

This paper describes and illustrates two ways of performing time-correlated gust-load calculations. The first is based on Matched Filter Theory; the second on Random Process Theory. Both approaches yield theoretically identical results and represent novel applications of the theories, are computationally fast, and may be applied to other dynamic-response problems. A theoretical development and example calculations using both Matched Filter Theory and Random Process Theory approaches are presented.

17. Key Words (Suggested by Author(s))

Matched Filter Theory
Random Process Theory
Gust Loads
Time-Correlated Gust Loads
Maximum Response

18. Distribution Statement

Unclassified - Unlimited

Subject Category - 05

19. Security Classif. (of this report)	20. Security Classif. (of this page)	21. No. of pages	22. Price
Unclassified	Unclassified	10	A02